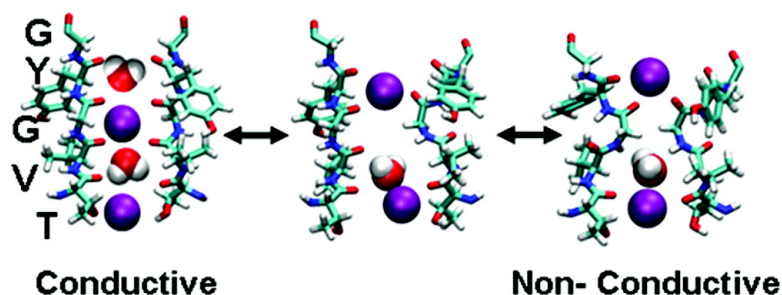Article

Conformational Changes and Gating at the Selectivity Filter of Potassium Channels

Carmen Domene, Michael L. Klein, Davide Branduardi, Francesco L. Gervasio, and Michele Parrinello

More About This Article

Additional resources and features associated with this article are available within the HTML version:

- Supporting Information
- Access to high resolution figures
- Links to articles and content related to this article
- Copyright permission to reproduce figures and/or text from this article

View the Full Text HTML

ACS Publications
High quality. High impact.

Conformational Changes and Gating at the Selectivity Filter of Potassium Channels

Carmen Domene,[*,†,§] Michael L. Klein,[‡] Davide Branduardi,[§]
Francesco L. Gervasio,[§] and Michele Parrinello[§]

*Physical and Theoretical Chemistry Laboratory, Department of Chemistry, University of Oxford,
South Parks Road, Oxford OX1 3QZ, U.K., Center for Molecular Modelling and Department of
Chemistry, University of Pennsylvania, 231 South 34th Street, Philadelphia, Pensylvannia
19104-6323, and Department of Chemistry and Applied Biosciences, ETH Zurich, USI -
Campus, via Giuseppe Buffi 13, 6900 Lugano, Switzerland*

Received March 11, 2008; E-mail: carmen.domene@chem.ox.ac.uk

Abstract: The translocation of ions and water across cell membranes is a prerequisite for many of life's processes. K^+ channels are a diverse family of integral membrane proteins through which K^+ can pass selectively. There is an ongoing debate about the nature of conformational changes associated with the opening and closing and conductive and nonconductive states of potassium (K^+) channels. These changes depend on the membrane potential, the K^+ concentration gradient, and large scale motions of transmembrane helices and associated residues. Experiments also suggest that local structural changes in the selectivity filter may act as the dominant gate referred to as C-type inactivation. Herein we present an extensive computational study on KirBac, which supports the existence of a physical gate or constriction in the selectivity filter (SF) of K^+ channels. Our computations identify a new selectivity filter structure, which is likely associated with C-type inactivation. Specifically, the four peptide chains that comprise the filter adopt an unusual structure in which their dihedrals alternate between left- and right-handed Ramachandran angles, which also justifies the need for conservation of glycine in the K^+ selectivity filter, since it is the only residue able to play this bifunctional role.

Introduction

The selectivity filter (SF) of K^+ channels is the crucial structural element controlling permeation and selectivity in these membrane protein architectures. Four identical subunits (see Figure 1) are symmetrically disposed to form the central pore, through which ions travel. Each contains a conserved signature peptide sequence: the TVGYG motif.[1] This sequence adopts an extended strand conformation where the carbonyl oxygens of the backbone point toward the lumen orchestrating the movements of ions in and out of the channel. Noticeably, glycine residues are absolutely conserved in the SF of all K^+ channels. The key carbonyl oxygens together with the side-chain hydroxyl oxygen of the threonine define four equally spaced ion-binding sites, which are commonly labeled S1−S4, from the extracellular to the intracellular region.[2] Another binding site, S0, has been proposed from molecular dynamics (MD) simulations[3] and crystallographic data.[1] Here, K^+ is stabilized by the carbonyl oxygens of the extracellular glycines and water from the milieu solution.[1] It has been shown that the most stable configurations of ions in the SF are S2/S4 and S1/S3 in the KcsA K^+

channel.[2,4] A low energetic barrier ($\sim$2−4 kcal/mol) between these two configurations allows rapid K^+ conduction through the SF.[2,4] In a low K^+ concentration, the SF structure is significantly different than that at high K^+ concentration.[1] Ions are absent at positions S2 and S3, and Val76 and Gly77 adopt new conformations. The average occupancy of the SF is one K^+ ion.[1] The ability of the SF to adopt two structures provides a built-in mechanism for adjusting to the high and low K^+ concentration that result from the channel gating.[1]

That the SF of K^+ channels might have the ability to act as a gate by switching between conducting and nonconducting states has long been hypothesized,[5] and recently new evidence has emerged.[6−8] This process, known as C-type inactivation, occurs with a wide range of rates on time scales ranging from tens of milliseconds to seconds.[9,10] It is generally much slower than the so-called N-type mechanism where an NH_2-terminal

† University of Oxford.
§ ETH Zurich.
‡ University of Pennsylvania.
(1) Zhou, Y.; Morais-Cabral, J. H.; Kaufman, A.; MacKinnon, R. *Nature* **2001**, *414*, 43–48.
(2) Berneche, S.; Roux, B. *Nature* **2001**, *414*, 73–77.
(3) Berneche, S.; Roux, B. *Biophys. J.* **2000**, *78*, 2900–2917.

(4) Aqvist, J.; Luzhkov, V. *Nature* **2000**, *404*, 881–884.
(5) Yellen, G. *Q. Rev. Biophys.* **1998**, *31*, 239–295.
(6) Cordero-Morales, J. F.; Jogini, V.; Lewis, A.; Vasquez, V.; Cortes, D. M.; Roux, B.; Perozo, E. *Nat. Struct. Mol. Biol.* **2007**, *14*, 1062–1069.
(7) Cordero-Morales, J. F.; Cuello, L. G.; Zhao, Y. X.; Jogini, V.; Cortes, D. M.; Roux, B.; Perozo, E. *Nat. Struct. Mol. Biol.* **2006**, *13*, 311–318.
(8) Bake, K. A.; Tzitzilonis, C.; Kwiatkowski, W.; Choe, S.; Riek, R. *Nat. Struct. Mol. Biol.* **2007**, *14*, 1089–1095.
(9) Marom, S.; Levitan, I. B. *Biophys. J.* **1994**, *67*, 579–589.
(10) Stuhmer, W.; Ruppersberg, J. P.; Schroter, K. H.; Sakmann, B.; Stocker, M.; Giese, K. P.; Perschke, A.; Baumann, A.; Pongs, O. *EMBO J.* **1989**, *8*, 3235–3244.

domain (ball domain) of the channel physically blocks the open pore.[11] Several lines of experimental evidence suggest that C-type inactivation involves a constriction within the mouth of the SF compromising interactions between different channel subunits.[12–16] There are also substantial effects of permeant ions in the C-type inactivation gating process.[12,17] In more recent studies, transitions to and from an inactivated state similar to C-type inactivation were proposed to depend on the carboxyl–carboxylate interaction between the Glu71 and Asp80 side chains in KcsA;[7,8,18] very informative crystal structures provided a glimpse of conformations available to this region of the channel during gating.[6,7]

Computational studies have suggested that conformational changes in the SF involving the Val residue of the TVGYG motif plays the principal role.[19] Specifically, Bernèche and Roux proposed a nonconductive state of broken symmetry, very stable compared to the time scales of ion translocation, and a free energy barrier of ∼11 kcal/mol to return the SF to its conductive conformation. The present computational studies revisit the nature of the conformational changes associated with transitions between conductive and nonconductive states of the selectivity filter. We have identified a new twofold symmetric conformation of the SF (Figure 1). This conformation was found while performing long metadynamics[20] and umbrella sampling trajectories[21] and confirmed by running a path based collective variable metadynamics run.[22]

Materials and Methods

Model System. The simulation system consisted of the 3.65 Å resolution KirBac1.1 channel (1P7B) embedded in a dioleoylphosphatidylcholine (DOPC) lipid bilayer. Each of the four subunits consists of 115 residues, from residue 40 to 154. An acetyl group was attached to the N-terminus residue to mimic the preceding peptide bond, and the C-terminal carboxylate was protonated. The program Whatif[23] was used to perform pK_A calculations to aid in assignment of side-chain ionization states, and on the basis of these calculations the side chains of Glu106 were protonated to form a diacid hydrogen bond with the carboxylate group of Asp115. Thus there is a shared proton between Asp115 and Glu106, homologous to that shared between Asp80 and Glu71 in KcsA.[24] The rest of the residues remained in their default ionization states. CHARMM27[25–27]

for proteins and lipids and Amber99SB[28] all atoms force fields as well as the TIP3P water model were used. Amber99SB has improved protein backbone parameters, in particular Gly backbone torsions relevant to this study. The parametrization of the DOPC molecule for Amber99SB was done following Jojart and Martinek.[29] The final equilibrated system contains in the KirBac1.1 simulation 55 776 atoms (10 249 TIP3P water molecules and 132 DMPC lipids, 19Cl⁻ and 19K⁺). The simulation methodology and protocol has been described previously.[30] One snapshot was chosen from those simulations as a starting point for the present studies, and the intracellular domain was removed. The reduced system was equilibrated in the NpT ensemble during 800 ps and a subsequent NvT ensemble during 200 ps with periodic boundary conditions and particle mesh Ewald electrostatics using the NAMD code.[31]

The same simulation system and simulation setup were used for the calculations performed using the path method. Parameters for the path runs, such as the choice of the atoms to be included in the path configuration (e.g., SF atoms, or SF backbone, or SF and a K⁺ ion, etc.), the interframe distance, the width and height of the gaussians, the frequency of deposition of gaussians, etc., were extensively tested and optimized on a subset of the full model. This subsystem contains the pore region and neighboring residues (Ala88–Ile138 for each monomer), three potassium ions, and 540 water molecules, accounting for a total of 4634 atoms. The initial coordinates were extracted from an equilibrium configuration of the full system. Backbone atoms except for those of the SF residues were harmonically restrained to their original positions with a 5 kcal/mol/Å² harmonic spring constant, and harmonic cylindrical boundary conditions were imposed with a radius of 25 Å and a length of 44 Å.

Metadynamics. The metadynamics technique in its direct formulation[32] was used to accelerate the movement of the K⁺ ions along the channel and to reconstruct the FES[33] of the permeation events. In this approach, the reaction coordinate is discouraged to remain fluctuating around the local minimum of, e.g., the reactant state, by adding a small Gaussian shaped potential to the reaction coordinate every few dynamics steps. The free energy reactant well will then become completely filled with Gaussian potentials during the MD run, allowing the system to escape the minimum via the lowest transition state to the next (product or intermediate) well, which will subsequently also be filled by Gaussians in the same fashion, and so forth. The FES of the system in question, including the transition states, can be obtained to arbitrary accuracy adding small enough potentials, by subtracting the sum of the added Gaussians, when the total free energy surface has been flattened.

Metadynamics was performed using as collective variables the relative distance of an ion along the pore axis (z-axis) with respect to the center of mass of the protein (CV $Z_i = z_i - z_{CM}$, $i = 1, 2$). Two K⁺ ions occupying simultaneously one of the sites of the SF were tracked. The height of the Gaussians was 0.72 kcal/mol, and the deposition time of hills was 0.5 ps. A multiple walker version of the metadynamics algorithm was used throughout.[34] Over 80 ns of enhanced sampling dynamics trajectories were generated.

As the final free energy surface must be symmetric with respect to the interchange of CVZ1 with CVZ2, the surface in Figure 2 has been produced averaging the upper triangle and the lower triangle of the metadynamics potential.

(11) Hille, B. *Ionic Channels of Excitable Membranes*, 3rd ed.; Sinauer Associates Inc.: Sunderland, MA, 2001.
(12) Liu, Y.; Jurman, M. E.; Yellen, G. *Neuron* **1996**, *16*, 859–867.
(13) Panyi, G.; Sheng, Z. F.; Tu, L. W.; Deutsch, C. *Biophys. J.* **1995**, *69*, 896–903.
(14) Panyi, G.; Deutsch, C. *J. Gen. Physiol.* **2006**, *128*, 547–559.
(15) Starkus, J. G.; Kuschel, L.; Rayner, M. D.; Heinemann, S. H. *J. Gen. Physiol.* **1997**, *110*, 539–550.
(16) Ogielska, E. M.; Zagotta, W. N.; Hoshi, T.; Heinemann, S. H.; Haab, J.; Aldrich, R. W. *Biophys. J.* **1995**, *69*, 2449–2457.
(17) Basso, C.; Labarca, P.; Stefani, E.; Alvarez, O.; Latorre, R. *FEBS Lett.* **1998**, *429*, 375–380.
(18) Cordero-Morales, J. F.; Cuello, L. G.; Perozo, E. *Nat. Struct. Mol. Biol.* **2006**, *13*, 319–22.
(19) Berneche, S.; Roux, B. I. *Structure* **2005**, *13*, 591–600.
(20) Laio, A.; Parrinello, M. *Proc. Natl. Acad. Sci. U.S.A.* **2002**, *99*, 12562–12566.
(21) Torrie, G. M.; Valleau, J. P. *Chem. Phys. Lett.* **1974**, *28*, 578–581.
(22) Branduardi, D.; Gervasio, F. L.; Parrinello, M. *J. Chem. Phys.* **2007**, *126*, 054103.
(23) Vriend, G. *J. Mol. Graphics* **1990**, *8*, 52.
(24) Ranatunga, K. M.; Shrivastava, I. H.; Smith, G. R.; Sansom, M. S. P. *Biophys. J.* **2001**, *80*, 1210–1219.
(25) MacKerell, A. D.; et al. *J. Phys. Chem. B* **1998**, *102*, 3586–3616.
(26) Feller, S. E.; Yin, D.; Pastor, S. E.; MacKerell, A. D. *Biophys. J.* **1997**, *73*, 2269–2279.
(27) Mackerell, A. D.; Feig, M.; Brooks, C. L. *J. Comput. Chem.* **2004**, *25*, 1400–1415.

(28) Hornak, V.; Abel, R.; Okur, A.; Strockbine, B.; Roitberg, A.; Simmerling, C. *Proteins* **2006**, *65*, 712–725.
(29) Jojart, B.; Martinek, T. A. *J. Comput. Chem.* **2007**, *28*, 2051–8.
(30) Domene, C.; Vemparala, S.; Klein, M.; Venien-Bryan, C.; Doyle, D. *Biophys. J.* **2006**, *90*, L1–L3.
(31) Kale, L.; Skeel, R.; Bhandarkar, M.; Brunner, R.; Gursoy, A.; Krawetz, N.; Philips, J.; Shinozaki, A.; Varadarajan, K.; Schulten, K. *J. Comput. Phys.* **1999**, *151*, 283–312.
(32) Laio, A.; Rodriguez-Fortea, A.; Gervasio, F. L.; Ceccarelli, M.; Parrinello, M. *J. Phys. Chem. B* **2005**, *109*, 6714–6721.
(33) Bussi, G.; Laio, A.; Parrinello, M. *Phys. Rev. Lett.* **2006**, 96.
(34) Raiteri, P.; Laio, A.; Gervasio, F. L.; Micheletti, C.; Parrinello, M. *J. Phys. Chem. B* **2006**, *110*, 3533–3539.
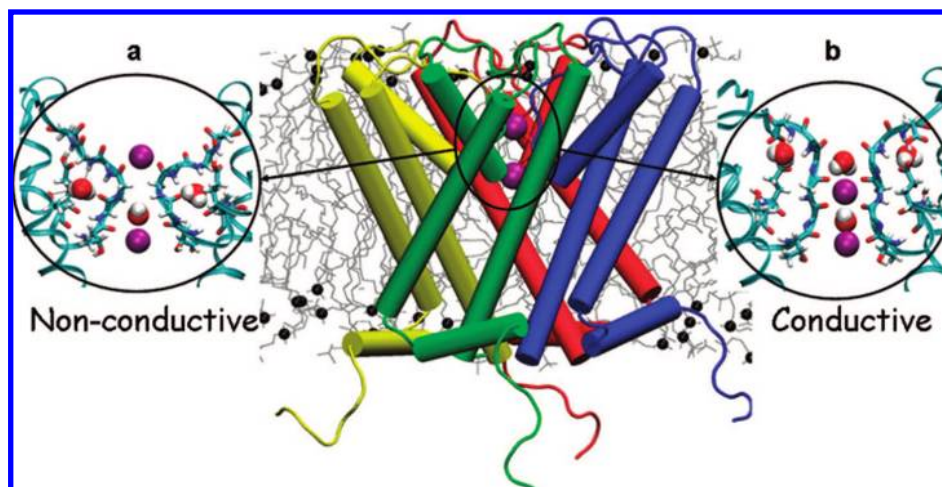
Figure 1. Representative nonconductive (a) and conductive (b) structures of the selectivity filter (SF). Shown is the full MD simulation system, consisting of a KirBac channel, whose subunit alpha-helices are rendered as colored sticks, embedded in a lipid bilayer, with individual lipids rendered as gray chains. For visual clarity in images a and b, atomic detail is given for only two out of the four subunits comprising the SF. K^+ ions are rendered as purple spheres, and water oxygen and hydrogen as red and white spheres, respectively. Only waters in the SF and those involved in the H-bond network are shown.
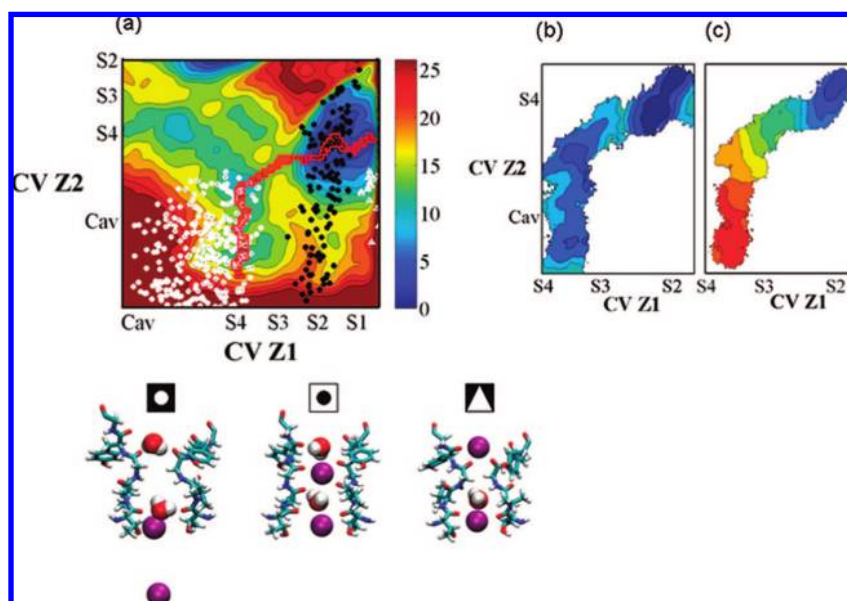

Figure 2. Free energy surface (FES) and corresponding SF configurations for K^+ ion translocation. (a) FES from metadynamics as a function of the positions of two K^+ ions. Only one complete diagonal of the symmetrized FES is shown for simplicity. Isosurfaces are one every 2 kcal/mol. Black and white dots and triangles correspond to structures with rmsd ≤ 0.6 Å from representative conductive and nonconductive structures (see main text), respectively. At first sight, the diagonal of this plot should be strongly forbidden (CVZ1 = CVZ2). However, two situations described in the main text bias the plot. (b) 2D umbrella sampling along the lowest free energy path that connects the minima in part a (in red) and (c) results using adaptive umbrella sampling starting with a perfect backbone configuration.

Umbrella Sampling. Umbrella sampling simulations were performed using the lowest free energy reaction path (LFEP) connecting the three minima obtained in the enhanced dynamics. The same two collective variables were used as reaction coordinates. The umbrella biasing potential was constructed from the two-dimensional FES computed with metadynamics by taking the potential along the LFEP.[35] This allows speeding up the calculations as the underlying free energy is expected to be roughly flat. Additionally, overlapping harmonic window potentials were applied along the path to enhance the sampling. The final converged free energy profiles were constructed by using the weighted histogram

analysis method.[36,37] Three different sets of umbrella sampling calculations were preformed: (1) a set of 233 biased simulations were run using a strip of 233 points on the LFEP, each of them exploring a slightly different range of conformations and configurations of K^+ ions (Figure 2b); (2) a set of 100 biased simulations were run using 100 points in a line on the LFEP and, as in the previous case, with each of them exploring a slightly different range of conformations and configurations of K^+ ions (data not shown); and finally (3) an adaptive umbrella sampling run, where biased simulations are run sequentially using the probabilities collected

(35) Ensing, B.; Klein, M. L. *Proc. Natl. Acad. Sci. U.S.A.* **2005**, *102*, 6755–6759.

(36) Kumar, S.; Bouzida, D.; Swendsen, R. H.; Kollman, P. A.; Rosenberg, J. M. *J. Comput. Chem.* **1992**, *13*, 1011–1021.
(37) Babin, V.; Roland, C.; Darden, T. A.; Sagui, C. *J. Chem. Phys.* **2006**, *125*, 204909.
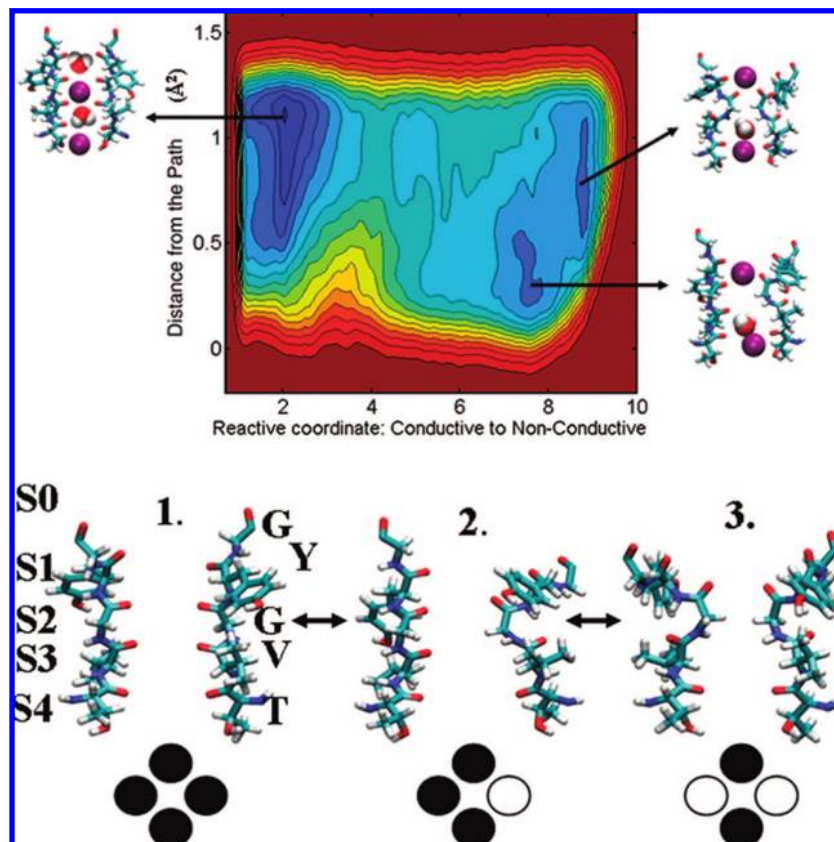
Figure 3. Free energy surface associated with selectivity filter (SF) conformational changes on going from a conductive to a nonconductive state. Surfaces are one per kcal/mol. For clarity, only two of the four subunits are shown. The complete transition takes place in two steps. (a) SF when the pore is occupied by two ions in sites S1/S3 or S2/S4. (b) Intermediate structure; only one of the four chains undergoes change. (c) Closed conformation. Below each figure there is a schematic representation of the tetrameric SF. Black and white circles correspond to a normal or kicked monomer.

after each stage to build improved biasing potentials that are used in the next run (Figure 2c). In the case of the strip, each umbrella was run for 50 ps, and in the other two cases, each umbrella was run for 150 ps, thus with a total of about 32 ns.

Path Based Method. In the path method[22] it is assumed that the transition to be studied can be described by a set of coordinates **R**, which are arranged to form a multidimensional vector representing the putative reaction coordinate. In the present study, the initial guessed path is a trajectory describing the conformational change observed in the metadynamics runs. Three structures from the metadynamics trajectories were selected to generate the initial path (see Figure 3), and a number of interpolated intermediates were obtained with the g_morh module of GROMACS in two steps: a first interpolation from structure 1 to structure 2 in Figure 3, and a second interpolation from structure 2 to structure 3 in Figure 3.

Two functions of the reaction coordinate **R** are introduced, namely *s* and *z*, which are able to describe the position of a point in configurational space relative to any preassigned path. *S* represents the progression along the predefined path and can be formalized as follows:

$$s(\mathbf{R}) = \frac{\sum_{i=1}^{P} i e^{-\lambda(R - R(i))^2}}{\sum_{i=1}^{P} e^{-\lambda(R - R(i))^2}} \qquad (1)$$

The corresponding *z* function, which defines the distance from the path, is

$$z(\mathbf{R}) = -\frac{1}{\lambda} \ln\left(\sum_{i=1}^{P} e^{-\lambda(\mathbf{R} - \mathbf{R}(i))^2}\right) \qquad (2)$$

where *i* is a discrete index ranging from 1 to *P* (1 to 10 in the present study). The aim is to estimate the low free energy path

that connects an initial state $\mathbf{R}_A$ to a final state $\mathbf{R}_B$. In this space an initial reaction coordinate is guessed. This initial reaction coordinate is expressed parametrically in the form **R**(*i*). The parametrization is such that $\mathbf{R}(0) = \mathbf{R}_A$ and $\mathbf{R}(1) = \mathbf{R}_B$. Herein, **R**(0) and **R**(1) correspond to the conductive and nonconductive conformations of the selectivity filter. Thus, the gating process is studied by following the evolution of the selectivity filter conformation; **R** is described by the Cartesian coordinate of the SF atoms involved in the process and the Cartesian coordinates of a K$^+$ ion. Only the heavy atoms of the SF and a potassium ion were included in the definition of **R**(*i*), and $(\mathbf{R} - \mathbf{R}(i))^2$ was calculated as a mean square displacement although other types of metrics might be considered. For this discrete representation to be meaningful it is necessary that the nodal points, **R**(*i*), are as equidistant as possible between successive frames and that λ is comparable to the inverse of mean square displacement between successive frames. Initially, the very first paths found will be close to the first trial path, but as $z(\mathbf{R})$ increases, alternatively paths which can be distinct from the initial one can be visited. Once we have chosen the initial path, metadynamics was run to reconstruct the FES(*s*,*z*). Each new path found is then optimized using a variational principle in the spirit of the finite temperature string method or nudget elastic band.

With the help of these two variables, *s* and *z*, the method combines features of approaches like metadynamics or umbrella sampling with those of path based methods.[38,39] This allows nonlocal searches in the space of paths to be performed. In contrast to metadynamics or umbrella sampling, the reactive path can be described by an arbitrary large number of variables and the calculation of energy profile along the path is easily computationally

(38) E, W.; Ren, W.; Vanden-Eijnden, E. *J. Chem. Phys.* **2007**, *126*, 164103.
(39) Henkelman, G.; Jonsson, H. *J. Chem. Phys.* **2000**, *113*, 9978–9985.

affordable. Added value with respect to other methods is the fact that several transition paths unrelated to the initial guess can be found. Reasonable results at a relatively low computational cost are readily obtained, thereby making possible its application to very large systems such as the ones described in this study.

Results and Discussion

Novel methodologies are required to identify and probe free energy barriers associated with rare events such as gating in ion channels. To overcome limitations inherent in brute force simulations, the metadynamics technique,[20] umbrella sampling,[21] and a path based collective variable method[22] have been used.

Initially, two K^+ ions were placed in the SF at canonical positions S1 and S3. The free energy surface (FES) obtained with metadynamics as a function of the position of the two K^+ ions is shown in Figure 2a. The FES as a function of these two collective variables (the relative position, CVZ1 and CVZ2, of the two different ions along the pore path) should be symmetrized because the probability of either ion to sample the free energy landscape is the same. Therefore, only one complete diagonal of the FES is shown for clarity where three minima can be distinguished. The lowest minimum on the FES corresponds to a configuration of ions in the SF in the S2/S4 arrangement. The other two minima identified (in cyan) correspond to configurations where the two ions involved in the collective variables can be found in S4 and the cavity with the rest of the sites is occupied by water molecules.

At first sight the diagonal of this plot should be strongly forbidden (CVZ1 = CVZ2). The fact that it is apparently not forbidden is mainly because at some point one K^+ ion interacts with Asp115 of one of the four monomers, once it has escaped to the extracellular solution. Then there is a cation−π interaction between this ion and the aromatic ring of Tyr113, at the back of the selectivity filter. Therefore, the *z* coordinates of the two ions can be the same, although the *x* and *y* coordinates are different. Two ions can also interchange positions when one of them is in the cavity and the other one is in S4. In this particular case, it could be said that there is double occupancy of S4. The channel can also have single ion occupancy (one ion inside the SF and the other one in the cavity or the extracellular solution). These situations bias the plot.

After analysis of the rmsd and the Ramachandran plots of the SF of different structures visited during the metadynamics trajectories (explored as a function of the position of the K^+ ions, namely CVZ1 and CVZ2), two interesting conformational regimes were detected. The first regime is the SF in the typical structure reported in experiments[40,41] and previous computational studies.[2,4] In what follows, this conformation[41] is going to be denoted as a "conductive structure" (Figure 1b). The second conformation of the filter has not been reported previously and corresponds to a nonconductive state (Figure 1a). Black dots in Figure 2a correspond to structures with rmsd values ≤ 0.6 Å from a representative conductive KirBac structure, where all the carbonyl oxygens of the TVGY motif are pointing toward the center of the pore coordinating the K^+ ions as described by its X-ray structure. The white dots and whites triangles in Figure 2a correspond to the new structure with rmsd values ≤ 0.6 Å from a representative nonconductive

KirBac structure. White circles correspond to the situation where ions involved in metadynamics are in S4 and the cavity and a water molecule occupies S1 and S3. S2 is not physically accessible in this new conformation. White triangles correspond to those configurations with ions in positions S1 and S4 and a water molecule in S3.

Two possible mechanisms lead to this conformational change. Initially, two K^+ ions occupy the SF and the pore is symmetric with all the carbonyl groups pointing toward the lumen. The transformation starts when one of the ions occupies S4 and the second ion in S2 oscillates between S2 and S1 sites. Then, one of the four chains flips (Figure 3). The "flickering" ion, the ion oscillating between sites S2 and S1, can subsequently depart toward the extracellular solution, after which the final nonconductive state is reached. This new conformation has only two backbone carbonyl oxygens from Val pointing toward the central pore, and site S2 disappears.

A slightly different mechanism is also observed during the metadynamics runs. In this second case, ions in S2 and S4 travel together toward the central cavity. If during this translocation the ion in S2 fluctuates between S2 and S3, the first backbone flip takes place. This change can lead to the fully nonconductive conformation if, subsequently, this ion travels toward S4. Eventually, another ion can approach the selectivity filter from the extracellular domain and sits in S1. Therefore, despite the different rearrangements of ions in these two processes, both of them lead the nonconductive conformation and the disappearance of S2.

In Figure 2a the energetics of the ion translocation along the pore of the channel is averaged with respect to conformational changes associated with pore occupancy. To separate these two factors, 2D umbrella sampling was performed along the lowest free energy path that connects the three minima on the FES (Figure 2a, in red) using configurations extracted from metadynamics (Figure 2b) and by adaptive umbrella sampling starting with a perfect backbone free to move (Figure 2c). The umbrella potentials are constructed on a strip of 233 points and by adaptive umbrella sampling starting with a perfect backbone free to move and using the last structure of the previous run as a starting point for the next umbrella. They were constructed from the FES computed with metadynamics since this already produces a flattened potential that speeds up convergence. The isosurfaces are one every 2 kcal/mol. Note that the red strip in Figure 2a traces the lowest free energy path between minima on the FES. The deep-blue regions are the most energetically favorable ones.

Since, in Figure 2b, the umbrella sampling runs have been performed using configurations extracted from metadynamics, where all possible backbone conformations are averaged, the difference in free energy between the metadynamics and the umbrella calculations yields approximately the work required for the conformational change, which is ~6−8 kcal/mol.

To confirm the above results, one of the mechanisms leading to the conformational change and associated thermodynamics was studied with a new path based method.[22] An initial path linking conductive and nonconductive structures was extracted from the metadynamics trajectory (Figure 1). In the definition of the path the positions of all SF heavy atoms and one K^+ inside the filter were included. Multiple runs were performed with two different force fields, CHARMM27 for protein and lipids and Amber99 SB.

During gating, the filter progresses through three stages. Figure 3 gives an account of the conformational changes that

(40) Doyle, D. A.; Cabral, J. M.; Pfuetzner, R. A.; Kuo, A.; Gulbis, J. M.; Cohen, S. L.; Cahit, B. T.; MacKinnon, R. *Science* **1998**, *280*, 69–77.

(41) Kuo, A.; Gulbis, J. M.; Antcliff, J. F.; Rahman, T.; Lowe, E. D.; Jochen, Z.; Cuthbertson, J.; Ashcroft, F. M.; Ezaki, T.; Doyle, D. A. *Science* **2003**, *300*, 1922–1926.
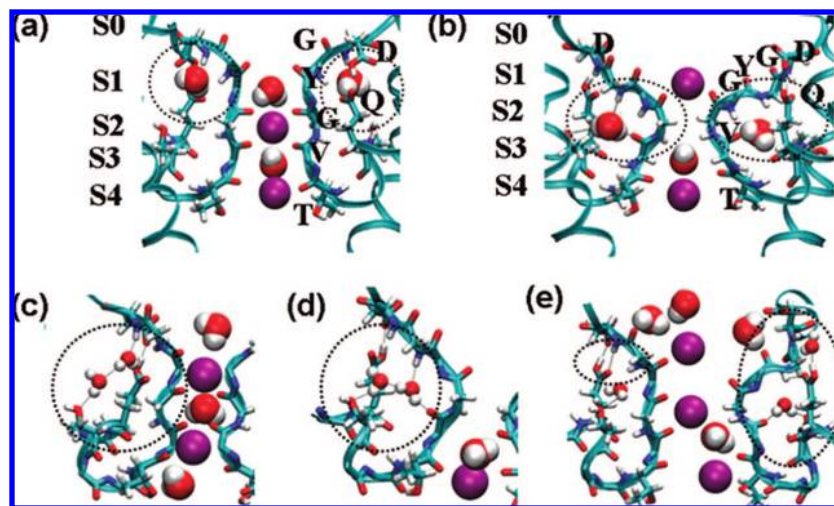
Figure 4. Atomic detail of the SF in a representative conductive and nonconductive structure. K$^+$ ions are represented as purple spheres. Water molecules in the SF and those at its back and involved in the H-bond network are also shown. Black lines link H-bonded atoms. Several situations are observed where just one water molecule is implicated (a and b) in the H-bond network or two water molecules are implicated (c and d). In the conductive state (a), the water molecule at the back of the SF is H-bonded to Glu106, Asp115, and Thr107, whereas, in the nonconducting state (b), the H-bond network is between the water molecule and Thr107, Val111, Tyr113, and Gly114. In some other occasions it is observed that the interaction between Glu106 and Asp115 can be broken (e right) or be directly formed in the absence of any water molecule (e left).

occur passing from a conductive to a nonconductive state and report the free energy surface (FES) as a function of the reactive coordinate and the distance from the set of coordinates. The barrier for the conformational transition is small, ~5−6 kcal/mol, in both force fields.

The conformational changes observed during this gating process lower the global symmetry of the structure from four- to twofold and involve a cooperative conformational change between K$^+$ ions and the SF residues. All four subunits are involved, and the intersubunit interactions are mediated through the ion-conducting pore and through direct side chain or backbone interactions. The conformational rearrangement of two out of the four opposite chains is asynchronous and caused by a transient asymmetric movement of two ions in the SF.

Unequivocally, the sequence of ion movements is coupled to the backbone conformations. The new structure never arises when ions occupy simultaneously S2 and S4 or S1 and S3 sites or when S2 is occupied either by an ion or by a water molecule. Glycine conservation and backbone flexibility are thus crucial characteristics of the SF.

As noted previously, the SF of KcsA is stabilized by a network of hydrogen bonds to the amide nitrogen atoms that points away from the pore, into the protein core.[1] The network includes a hydrogen bond between the carboxylic group of Glu71 and that of Asp80 and a buried water molecule present in the crystal structure. Similarly, in KirBac1.1 a hydrogen bond network exits organized around Glu106 and Asp115. Water molecules were not present in the crystal structure of KirBac1.1 at the back of the SF. However, during the MD trajectory, water molecules arrived at these sites at different times, and up to three of them sometimes occupy the volume at the back of the SF. A similar hydrogen bond network to that of KcsA is observed among Glu106, Asp115, and these water molecules. Figure 4a and 4b show the atomic detail of the SF of the KirBac1.1 channel in the conductive and nonconductive conformations, respectively. These structures are remarkably different. In particular, Val111 has adopted a new configuration in the nonconductive conformation, and its backbone carbonyl points toward the back of the SF. This carbonyl group is part

of a hydrogen bond network connecting one (Figure 4a and b) or two water molecules (Figure 4c and d) with the NH of Gly114, the OH of Thr107, and the OH−Tyr113 group of the nearby monomer. Thr107 is not fully conserved in the Kir family of K$^+$ channels, though it is also conserved in KcsA, MthK, and Shaker channels for instance. Nevertheless, experimental evidence is reported whereby mutations of such analogous residues to Thr107, in the P-loop in the Kir family, alter the conducting properties of the channel.[42] During the present simulations, several events are observed where a water molecule is simultaneously hydrogen bonded to both Glu106 and Asp115 (Figure 4e, right), Glu106 and Asp115 form a direct hydrogen bond (Figure 4e, left), and on some other occasions, the H-bond between Glu106 and Asp115 is broken, so that the Asp residues become more accessible to the bulk solution (Figure 4e, right).

The principal mission of ion channels is to regulate the flow of ions across membranes. The data presented herein support the experimental hypothesis that the SF itself can be a gate. The present finding is also consistent with a model whereby the conformational changes during the inactivation proceeds by a multistep process and where the presence or absence of K$^+$ ions in particular sites of the SF is a key factor in such a mechanism.[19] The nonconducting state described herein will be able to regulate cell function by modulating excitability through its coupled effects on the global activation gating.

(42) Proks, P.; Capener, C. E.; Jones, P.; Ashcroft, F. *J. Gen. Physiol.* **2001**, *118*, 341–353.

Supporting Information Available: Complete ref 25; (Figure 1S) Representation of the subsystem used to tune the parameters for the path calculations; (Figure 2S) Free energy surface (FES) from metadynamics for K^+ ion translocation as a function of the positions of two K^+ ions; and (Figure 3S) Free energy surface associated to SF conformational changes on going from a conductive to a nonconductive state using the CHARMM27 force field for protein and lipids. This material is available free of charge via the Internet at http://pubs.acs.org.

JA801792G